

Published in final edited form as:

J Colloid Interface Sci. 2015 January 1; 437: 140–146. doi:10.1016/j.jcis.2014.09.020.

Facilitated Preparation of Bioconjugatable Zwitterionic Quantum Dots Using Dual-Lipid Encapsulation

Robert Shrake^{‡,a,b}, Violeta G. Demillo^{‡,a,b}, Mojtaba Ahmadiantehrani^c, Xiaoshan Zhu^{*,a,b}, Nelson G. Publicover^{a,b,d}, and Kenneth W. Hunter Jr.^{b,d}

^aDepartment of Electrical and Biomedical Engineering, University of Nevada, Reno, NV, USA

^bBiomedical Engineering Program, University of Nevada, Reno, NV, USA

^cDepartment of Chemical and Materials Engineering, University of Nevada, Reno, NV, USA

^dDepartment of Microbiology and Immunology, University of Nevada, Reno, NV, USA

Abstract

Zwitterionic quantum dots prepared through incorporated zwitterionic ligands on quantum dot surfaces, are being paid significant attention in biomedical applications because of their excellent colloidal stability across a wide pH and ionic strength range, antifouling surface, good biocompatibility, etc. In this work, we report a dual-lipid encapsulation approach to prepare bioconjugatable zwitterionic quantum dots using amidosulfobetaine-16 lipids, dipalmitoyl-sn-glycero-3-phosphoethanolamine lipids with functional head groups, and CuInS₂/ZnS quantum dots in a tetrahydrofuran/methanol/water solvent system with sonication. Amidosulfobetaine-16 is a zwitterionic lipid and dipalmitoyl-sn-glycero-3-phosphoethanolamine, with its functional head, provides bioconjugation capability. Under sonication, tetrahydrofuran/methanol containing amidosulfobetaine-16, dipalmitoyl-sn-glycero-3-phosphoethanolamine, and hydrophobic quantum dots are dispersed in water to form droplets. Highly water-soluble tetrahydrofuran/methanol in droplets is further displaced by water, which induces the lipid self-assembling on hydrophobic surface of quantum dots and thus forms water soluble zwitterionic quantum dots. The prepared zwitterionic quantum dots maintain colloidal stability in aqueous solutions with high salinity and over a wide pH range. They are also able to be conjugated with biomolecules for bioassay with minimal nonspecific binding.

Keywords

Zwitterionic quantum dots; lipids; encapsulation; CuInS₂/ZnS; surface modification; colloidal stability; bioconjugation

© 2014 Elsevier Inc. All rights reserved.

*To whom correspondence should be addressed. xzhu@unr.edu. Phone: 1-775-682-6298. Fax: 1-775-784-6627.

‡Equal contribution to this work

Publisher's Disclaimer: This is a PDF file of an unedited manuscript that has been accepted for publication. As a service to our customers we are providing this early version of the manuscript. The manuscript will undergo copyediting, typesetting, and review of the resulting proof before it is published in its final citable form. Please note that during the production process errors may be discovered which could affect the content, and all legal disclaimers that apply to the journal pertain.

INTRODUCTION

Although quantum dots (QDs) synthesized in organic solvents at high temperature are typically of high quality with respect to photoluminescence, brightness and stability against photobleaching, they are not soluble in aqueous solutions. Appropriate surface modification of QDs is a prerequisite for further biomedical applications, not only to render them water-dispersible but also to provide functional groups for subsequent bioconjugation with biological moieties [1–3].

In two common surface modification strategies for QDs (ligand exchange and polymer encapsulation) [3], polyethylene glycol (PEG) chains, due to their good steric stabilization capability, are often incorporated into the hydrophilic portion of ligands or polymers to achieve enhanced QD colloidal stability [3–7]. Since a PEG end can be further modified to have functional groups such as amine, carboxyl and maleimide groups, PEG coated QDs (PEG-QDs) can be produced with bioconjugation capabilities. In spite of these merits, PEG-QDs constructed with functional groups are expensive, and have also been reported to tend to aggregate in high salinity buffers [8].

The use of zwitterionic groups such as carboxybetaine and sulfobetaine has been presented as alternatives to PEG [8–13]. A zwitterion is a neutral molecule with both a positive and a negative electrical charge. The positive and negative charges form an inner electrical field between them. The two charges are very close and thus, the inner electrical field is strong enough to attract water molecules to align with the electrical field [14]. The attracted water molecules form a hydration layer. The hydration layer is very stable and remains almost unperturbed under harsh conditions such as high/low pHs and high salinity. When zwitterions are coated on QD surfaces, the hydration layer of each zwitterion encapsulates QDs. The hydration layer repulsion between QDs prevents QD aggregation. Moreover, the hydration layer repulsion is less susceptible to pH or ionic strength effects compared to the electrostatic repulsion of surfaces with a single charged group [12]. As a result, zwitterionic QDs (ZW-QDs) achieve good colloidal stability in aqueous solutions with wide pHs and/or high salinity. In addition, recent studies have revealed that ZW-QDs present minimal nonspecific binding and good biocompatibility with cells or tissues [15–16]. Thus, it is of interest to develop ZW-QDs.

To prepare ZW-QDs, zwitterionic groups are usually coupled to thiol ligands such as dihydrolipoic acid [8–12], and these coupled ligands are further exchanged with hydrophobic ligands on QD surfaces due to the high binding affinity of thiols to Zn atoms on the surface. To provide functional sites for bioconjugation, thiol ligands with head groups such as amines and carboxyls were simultaneously synthesized and applied in small portions for ligand exchange during QD surface modification. Although these bioconjugatable ZW-QDs are meritorious for biomedical applications, the synthesis of the coupled ligands involves many complicated and costly steps. In addition, thiols are apt to oxidize in the presence of oxygen and therefore lose their binding affinity, deteriorating QD stability [3, 5–6]. More specifically, in the case of CuInS₂/ZnS QDs, ligand exchange is less favorable compared to tri-octylphosphine oxide stabilized QDs such as CdSe/ZnS, because CuInS₂/ZnS QDs are normally coated with dodecanethiol resulting from production, and

dodecanethiol has a higher binding affinity to QD surface Zn atoms than tri-octylphosphine oxide [17]. On the other hand, several reports describe the preparation of ZW-QDs through encapsulating single or multiple QDs in zwitterionic amphiphilic polymers [17–21]. However, the ZW-QD preparation requires multiple time-intensive steps including an overnight air-dry from chloroform. Moreover, the bioconjugation capability of the ZW-QDs using regular crosslinking reagents has not been reported.

Recently, the interaction between lipids and nanoparticles has gained considerable attention. These studies disclose the effects of nanoparticle surface charge, composition and size on the final morphology of nanoparticle-lipid complexes [22]. They also open the prospect for engineering novel lipid-nanoparticle assembled biomaterials for various biological or biomedical applications such as bioassay, drug delivery and so on [22–26]. In this work, we report a facilitated method for the preparation of bioconjugatable ZW-QDs using dual-lipid encapsulation. The lipid encapsulation on QDs is based on hydrophobic-hydrophobic bonding between lipids and QDs. The lipids are amidosulfobetaine-16 (ASB-16) and dipalmitoyl-sn-glycero-3-phosphoethanolamine (DPPE) with functional heads (e.g., carboxyl or maleimide), respectively. ASB-16 is a zwitterionic lipid, and DPPE with functional head provides bioconjugation capabilities. The dual-lipid encapsulation on QDs is implemented through a quick solvent exchange process. The preparation process is illustrated in Figure 1. QDs, ASB-16 and DPPE lipids dissolved in a highly water-miscible organic liquid are injected into water under sonication. With appropriate conditions (e.g., sonication magnitude, lipid to QD molar or mass ratio, etc.), organic droplets containing ASB and DPPE lipids and QDs are dispersed in water. Because the organic liquid is highly water-soluble with low viscosity, water quickly displaces organic liquid in the droplets. During solvent displacement, the hydrophobic portion of lipids intercalates with the hydrophobic ligands on the QD surface while exposing the hydrophilic portion to aqueous solutions. After solvent displacement, organic liquids dissolved in water are removed by rotary evaporation. In this preparation process, the selection of water-miscible organic liquid is critical. Although tetrahydrofuran (THF) is highly soluble in water, ASB and DPPE lipids do not dissolve well in THF. To overcome this challenge, we introduce methanol as a co-solvent to THF. The THF-methanol system represents a powerful combination to dissolve QDs and lipids (ASB and DPPE). Moreover, both THF and methanol are water-miscible and can be easily removed by rotary evaporation due to their low boiling points. Compared to ligand exchange and polymer encapsulation for QD surface modification, this approach is simple, fast and cost effective in production by avoiding complicated or long-time fabrication steps and adopting low-cost lipids. To our knowledge, this dual-lipid-encapsulation based method to prepare bioconjugatable ZW-QDs is novel.

EXPERIMENTAL METHODS

Materials and Apparatus

Copper(I) Iodide (99.999%), Sulfur (>99.99%), Trioctylphosphine (TOP, 90%), Methanol (99.93%), Hexadecanediol (90%), and 1-Octadecene (ODE, 90%) were purchased from Sigma Aldrich. 1-Dodecanethiol (DDT, 98%), Indium (III) Acetate (99.98%), and Zinc Stearate were purchased from Alfa Aesar. Amidosulfobetaine-16 (ASB-16, >99%) was

purchased from G-Biosciences. Tetrahydrofuran (THF, >99%), Ethanol (>99%), Chloroform (>99.9%), and Hexane (95%) were purchased from Pharmco-AAPER. N-Glutaryl-L- α -phosphatidylethanolamine (DPPE-GLU) (>97%) and N-(3-Maleimide-1-oxopropyl)-L- α -phosphatidylethanolamine (DPPE-MAL) (>95%) were purchased from NOF America Corporation. Biotin Magnetic Beads (4.3 μ m in diameter, 1% w/v) were purchased from Spherotech. Phosphate buffered saline (PBS), ethylenediaminetetraacetic acid (EDTA), Traut's Reagent and Neutravidin were purchased from Thermo Scientific. Bovine serum albumin (BSA) was from MP Biomedicals. All chemicals were used as purchased from the manufacturer without further purification.

Infrared (IR) spectra of lipids and quantum dots (QDs) were collected using an Fourier transform infrared (FT-IR) spectrometer (Perkin-Elmer Frontier) with Spectrum 10 software and the Universal ATR Sampling Accessory. The ultraviolet and visible (UV-Vis) spectra of materials were obtained with a UV-Vis spectrometer (UV-2450 from Shimadzu). Photoluminescence spectra of QDs in organic-phase and aqueous-phase were acquired using a spectrophotometer (RF-5301PC from Shimadzu). Photoluminescence intensity of QDs in various buffers was obtained using a microplate reader (PerkinElmer 2030 equipped with a 655 nm emission filter and a 405 nm excitation filter). Transmission electron microscopy (TEM) images were acquired using a JEOL analytical transmission electron microscope (model JEM 2100F operated with a 200 kV acceleration voltage). Probe sonication was performed with a Misonix ultrasonic processor (QSonica S-4000) equipped with a microtip.

CuInS₂/ZnS QDs Preparation

0.25 mmol Copper (I) Iodide and 0.25 mmol Indium (III) acetate were added in 4 mL DDT in a three-necked round bottom flask. This solution was heated to 140 °C under vacuum for 30 min until the solution became clear. The temperature of the flask solution was then increased to 240 °C under Argon. The solution was refluxed for the growth of CuInS₂ core nanocrystals. After 30 min growth, the solution was cooled to room temperature and 4 mL ODE were added. For ZnS shell growth, this core growth solution was heated to 140 °C under vacuum for 30 min and then to 240 °C under Argon. 0.4 M sulfur precursor was prepared dissolving sulfur in DDT and TOP, and 0.4 M zinc precursor was prepared by dissolving zinc stearate in ODE. Both zinc and sulfur precursors were injected in sequence 6 times to the core growth solution at 240 °C in 1.0 mL portions at 20 min intervals. After reactions were complete, mixtures were cooled down to room temperature under Argon and CuInS₂/ZnS QDs were purified using hexane and ethanol, and dried under vacuum.

Preparation of Bionconjugatable Zwitterionic Quantum Dots (ZW-QDs)

0.6 mg hydrophobic CuInS₂/ZnS QDs, 2.22 mg ASB-16, and 0.99 mg DPPE-GLU were dissolved in 0.8 mL THF:methanol (4:1 in volume). This solution was then injected into 3.5 mL cold water within one min under sonication (a micro sonication tip with 10 W output power). After injection, the solution was vacuum dried for 30 min to remove methanol and THF using a rotary evaporator. After rotary evaporation, the ZW-QDs were washed three times using an ultrahigh centrifuge (200,000 ~ 500,000 g) and then passed through a 300K MWCO filter (with ~ 35 nm pore size).

Conjugation of ZW-QDs with Neutravidin and Neutravidin-Biotin Assay

ZW-QDs were prepared using DPPE-maleimide and ASB-16 in the molar ratio of 1:4, and suspended in 300 μL PBS pH 6 with 5 mM EDTA. The thiolation of Neutravidin was completed by dispersing 2.5 nmol of Neutravidin in 100 μL of PBS (pH8, 5 mM EDTA) with 25 nmol of Traut's reagent. 150 μL of the prepared ZW-QDs were incubated with thiolated Neutravidin for 2 hr. After incubation, the ZW-QDs were washed five times in PBS pH7.5 using a 100K MWCO centrifugal filter and then re-suspended in 150 μL PBS pH7.5 as conjugate stock. The other half of the prepared ZW-QDs (150 μL) was not conjugated and used as a control.

Two μL of biotinylated magnetic microbeads (4.5 μm diameter, 4×10^8 beads/mL) were placed in each well of a microplate. Different volumes of the conjugate stock solution were loaded into wells, and PBS pH7.5 buffer was used to bring the total volume in each well to 50 μL . The unconjugated ZW-QDs stock solution under the same dilutions was used as controls. The microplate was vortexed at room temperature for 30 min, and then the magnetic microbeads in each well were washed using PBS pH7.2 with 1% BSA and dispersed in 50 μL of PBS pH7.2 with 0.1% BSA. The fluorescence signals of the suspended microbeads in wells were measured using a microplate reader with a 405 nm excitation filter and a 655 nm emission filter. The experiments were performed in triplicate.

RESULTS AND DISCUSSION

Although cadmium-based QDs such as CdSe/ZnS can also be adopted in these methods, CuInS₂/ZnS QDs have recently gained considerable attention due to a lack of handling hazardous cadmium materials during synthesis and their low toxicity in biomedical applications [27–31]. Thus, CuInS₂/ZnS QDs emitting red fluorescence (~ 670 nm) were synthesized and used in the preparation of ZW-QDs. The synthesis and characterization of CuInS₂/ZnS QDs have been previously reported [31]. The hydrophobic ligands on CuInS₂/ZnS QDs are dodecanethiol. To prepare ZW-QDs, the hydrophobic CuInS₂/ZnS QDs together with ASB-16 and DPPE dissolved in THF/methanol were dispersed in water to form droplets under sonication. Since THF/methanol are highly soluble in water, they are quickly displaced by water in the droplets. The solvent displacement induces the lipid self-assembling on hydrophobic surface of QDs and thus forms water soluble ZW-QDs. After a size-exclusion process (ZW-QD centrifugation through a 300K MWCO filter with ~35 nm pore sizes), the ZW-QDs flowing through the filter were collected for further use. TEM images of the hydrophobic QDs and the collected ZW-QDs are shown in Figure 2. It can be seen that ZW-QDs present a size no more than 20 nm and they are larger than hydrophobic QDs. The size difference suggests multiple hydrophobic QDs per encapsulation.

Figure 3 shows the FT-IR spectra of materials used in producing ZW-QDs and the resultant ZW-QDs. It can be seen that the peaks in the spectra of hydrophobic QDs and ASB-16 and DPPE-GLU are represented in the ZW-QDs. For instance, the spectra of ASB-16 and DPPE-GLU show peaks at around 1036 cm^{-1} , 1180 cm^{-1} and 1740 cm^{-1} , respectively. The peaks at approximately 1180 cm^{-1} and 1036 cm^{-1} are from the S=O stretching vibration of the sulfo group in ASB-16. The C=O peak at around 1740 cm^{-1} is due to the ester group present

in DPPE [32]. These peaks are not observed in the spectrum of QDs but appear in dual-lipid encapsulated ZW-QDs. These changes clearly indicate that the lipids are attached to QDs.

Note that during the preparation of ZW-QDs, the masses of ASB-16 and DPPE-GLU were tuned as shown in Table 1 in order to investigate the lipid mass effect on ZW-QD absorption/emission spectra and quantum yield. In the mass tuning, the molar ratio between ASB-16 and DPPE-GLU was always kept at 4:1. Figure 4 shows the absorption and photoluminescence emission spectra of hydrophobic QDs and ZW-QDs prepared under different mass ratios of QDs to total lipids. As shown in Figure 4, phase transfer causes a red-shift of all PL emission spectra together with the 40–50% decrease in quantum yield of QDs, compared to that of QDs in THF. Moreover, as the mass ratio of QDs to total lipids decreases, the PL emission spectra of resultant ZW-QDs show a slight blue-shift and quantum yield enhancement. The red-shift and the quantum yield drop after the phase transfer may be caused by the formation of QD clusters (Figure 2) in the dual-lipids encapsulation process. In this case, since the QDs are packed closely, the emission photons from smaller QDs are absorbed by larger QDs to emit a longer wavelength (a Förster resonance energy transfer process). Moreover, the formation of clusters reduces total QD excitation and emission surface area, resulting in a quantum yield drop. In addition, it was found that ASB-16 and DPPE lipids absorb light over a wide wavelength range (Figure S1 in the supplementary materials). Lipids could absorb excitation photons directed at QDs and emission photons from QDs, and therefore contribute to the red spectral shift and the quantum yield decrease.

The slight blue shift and the quantum yield enhancement when the mass ratio of QDs to the total lipids is decreased may be attributed to fewer QDs per cluster due to more lipids in the preparation process. As the mass of lipids increases (or the mass ratio of QDs to lipids decreases), more lipids (surfactants) can interact with QDs. When the mixture of QDs and lipids in THF/methanol were injected into water, more lipids should lower the surface tension between water and THF/methanol. Under sonication, it is believed that the lowered surface tension facilitates the dispersion of the organic solution into water and organic solvent droplets could contain fewer QDs on average. As a result, the overall emission spectrum of the formed clusters moves towards that of single QDs in THF (spectral blue shift). Fewer QDs per cluster also causes quantum yield enhancement because total QD excitation and emission surface area is increased.

The stability of the prepared ZW-QDs was tested under various conditions by monitoring their photoluminescence intensity over time [8, 33–34]. As shown in Figure 5(a), the photoluminescence intensity and hence stability of these QDs was maintained in PBS with pH 3–11, pure water, a 1M NaCl solution, and 10% FBS over 48 hours at room temperature. Figure 5(b) shows images of the solutions with ZW-QDs under the same conditions after 48 hours. The ZW-QDs in glass vials were also illuminated with 405 nm UV light (bottom panel in Figure 5(b)) and room light (top panel in Figure 5(b)), respectively. It is clear that the dispersions are relatively stable at room temperature for at least 48 hours in solutions over a wide range of pH and in high-salinity as well as in physiological media. As evident from the homogeneous fluorescence of samples, no precipitates or significant photoluminescence intensity decreases were observed. The stability of the dual-lipid

encapsulated QDs offers a great deal of flexibility for their applications in biological or biomedical experiments. Additionally, the samples shown in Figure 5(b) were monitored over a week. No precipitates or significant photoluminescence intensity decreases were observed over this time. The ZW-QDs were also shown to be stable in water at 4 C over weeks (Figure S2 in the supplementary materials). For long-term storage of ZW-QDs, drying the QDs, storing and then re-suspending them in appropriate solutions before use could be a feasible approach.

To further investigate the effects of ASB-16 and DPPE on QD stability, QDs coated with only ASB-16 or with only DPPE were prepared. Due to their anionic surface, DPPE-coated QDs rely on electrostatic repulsion to achieve colloidal stability. Since high salt concentration (or salinity) can effectively alter electrostatic repulsion and thus stability by changing the cationic or anionic surface net charge, DPPE-coated QDs were suspended in 1M NaCl solution. After suspension, white precipitates were observed. Figure S3 in the supplementary materials clearly shows the instability of DPPE-coated QDs in high salinity. As a comparison, ASB-coated QDs were also suspended in 1M NaCl, and no precipitates or significant PL intensity decreases were observed. It can be seen that anionic lipid DPPE cannot ensure the QD stability in high salinity but zwitterionic lipid ASB can. The images in Figure S3 and Figure 5 suggest that the colloidal stability of dual-lipid encapsulated QDs is afforded by zwitterionic ASB-16 especially in 1M NaCl solution.

ASB-16 is a zwitterionic detergent with a sulfobetaine head. The sulfobetaine does not have a function group for bioconjugation using cross linking chemistry. To achieve bioconjugation, a generic approach is to introduce a portion of functional ligands mixed with zwitterion ligands [8, 34]. Functional ligands possessing amine, carboxyl, maleimide, and other functional groups can help the surface to conjugate with target biomolecules. DPPE lipids with functional groups were introduced for this purpose. To demonstrate the bioconjugation capability of the produced ZW-QDs, a Neutravidin-biotin assay using biotinylated magnetic microbeads and Neutravidin conjugated ZW-QDs was performed, as illustrated in Figure 6(a). In this assay, the biotin molecules on magnetic beads can specifically bind with Neutravidin molecules. ZW-QDs prepared using ASB-16 and DPPE-maleimide were conjugated with thiolated Neutravidin through maleimide-thiol reaction. To verify that Neutravidin was conjugated on ZW-QD surfaces, biotinylated magnetic beads were incubated with serial dilutions of Neutravidin-conjugated ZW-QDs from the stock suspension. Figure 6(b) shows the photoluminescence responses of the biotinylated magnetic microbeads after their incubation with the conjugates. As controls, the photoluminescence responses of the biotinylated magnetic microbeads after their incubation with non-conjugated ZW-QDs under the same concentrations were measured. For each concentration, the photoluminescence response for non-conjugated ZW-QDs is obviously lower than that of conjugated ZW-QDs, and similar to the background of magnetic microbeads. Thus, it is clear that the prepared ZW-QDs can be specifically conjugated with biomolecules, and they also produce minimal nonspecific-binding to magnetic microbead surfaces.

CONCLUSION

A dual-lipid encapsulation approach has been introduced to prepare bioconjugatable ZW-QDs. These ZW-QDs have been shown to be stable in solutions over a wide range of pH and with high salinity. They were also shown to conjugate with Neutravidin for biotin-Neutravidin assays with minimal nonspecific-binding. Compared to other approaches (ligand exchange or polymer encapsulation), this dual-lipid encapsulation method is simple, fast and cost effective. The developed surface modification approach can be applied for the phase transfer of many other hydrophobic nanoparticles such as oleic acid coated Fe₃O₄ magnetic particles. Bioconjugatable zwitterionic nanocomposites integrating both QDs and magnetic nanoparticles may also be fabricated using this approach for multimodal bioimaging. We believe that the unique surface modification and phase transfer approach opens an avenue for the produced nanocapsules to serve as a powerful platform incorporating other agents of interest such as therapeutic drugs in their hydrophobic core or linking biomolecular probes on their hydrophilic shell for broad biological or biomedical applications.

Supplementary Material

Refer to Web version on PubMed Central for supplementary material.

Acknowledgments

This research was supported by the National Institute of Health via grant #1P20GM103650-01. The authors acknowledge Professor Gregory Pari in the Department of Microbiology and Immunology at the University of Nevada Reno for technical support.

REFERENCES

1. Bruchez M Jr, Moronne M, Gin P, Weiss S, Alivisatos AP. *Science*. 1998; 281:2013–2016. [PubMed: 9748157]
2. Resch-Genger U, Grabolle M, Cavaliere-Jaricot S, Nitschke R, Nann T. *Nat. Methods*. 2008; 5:763–775. [PubMed: 18756197]
3. Sperling RA, Parak WJ. *Phil. Trans. R. Soc. A*. 2010; 368:1333–1383. [PubMed: 20156828]
4. Uyeda HT, Medintz IL, Jaiswal JK, Simon SM, Mattoussi H. *J. Chem. Soc.* 2005; 127:3870–3878.
5. Susumu K, Uyeda HT, Medintz IL, Pons T, Delehanty JB, Mattoussi H. *J. Am. Chem. Soc.* 2007; 129:13987–13996. [PubMed: 17956097]
6. Mei BC, Susumu K, Medintz IL, Delehanty JB, Mountziaris TJ, Mattoussi H. *J. Mater. Chem.* 2008; 18:4949–4958.
7. Tong S, Hou S, Ren B, Zheng Z, Bao G. *Nano Lett.* 2011; 11:3720–3726. [PubMed: 21793503]
8. Muro E, Pons T, Lequeux N, Fragola A, Sanson N, Lenkei Z, Dubertret B. *J. Am. Chem. Soc.* 2010; 132:4556–4557. [PubMed: 20235547]
9. Muro E, Fragola A, Pons T, Lequeux N, Ioannou A, Skourides P, Dubertret B. *Small*. 2012; 8:1029–1037. [PubMed: 22378567]
10. Susumu K, Oh E, Delehanty JB, Blanco-Canosa JB, Johnson BJ, Jain V, Hervey WJ IV, Algar WR, Boeneman K, Dawson P, Medintz I. *J. Am. Chem. Soc.* 2011; 133:9480–9496. [PubMed: 21612225]
11. Kim D, Chae M, Joo H, Jeong I, Cho J, Lee C. *Langmuir*. 2012; 28:9634–9639. [PubMed: 22607014]

12. Liu X, Huang H, Liu G, Zhou W, Chen Y, Jin Q, Ji J. *Nanoscale*. 2013; 5:3982–3991. [PubMed: 23546384]
13. Wei H, Insin N, Lee J, Han H, Cordero J, Liu W, Bawendi M. *Nano Lett*. 2012; 12:22–25. [PubMed: 22185195]
14. Schlenoff JB. *Langmuir*. 2014; 30:9625–9636. [PubMed: 24754399]
15. Park J, Nam J, Won N, Jin H, Jung S, Jung S, Cho S, Kim S. *Adv. Funct. Mater*. 2011; 21:1558–1566.
16. Breus VV, Heyes CD, Tron K, Nienhaus GU. *ACS Nano*. 2009; 3:2573–2580. [PubMed: 19719085]
17. Booth M, Peel R, Partanen R, Hondow N, Vasilca V, Jeuken LJC, Critchley K. *RSC Advances*. 2013; 3:20559–20566.
18. Yezhelyev MV, Qi L, O'Regan RM, Nie S, Gao X. *J. Am. Chem. Soc*. 2008; 130:9006–9012. [PubMed: 18570415]
19. Qi L, Gao X. *ACS Nano*. 2008; 2:1403–1410. [PubMed: 19206308]
20. Bagalkot V, Gao X. *ACS Nano*. 2011; 5:8131–8139. [PubMed: 21936502]
21. Gao, X. US Patent. US8063131 B2.
22. Schulz M, Olubummo A, Binder WH. *Soft Matter*. 2012; 8:4849–4864.
23. Gopalakrishnan G, Danelon C, Izewska P, Prummer M, Yves Bolinger P, Geissbuhler I, Demurtas D, Dubochet J, Vogel H. *Angew. Chem. Int. Ed*. 2006; 45:5478–5483.
24. Thaxton CS, Daniel WL, Giljohann DA, Thomas AD, Mirkin CA. *J. Am. Chem. Soc*. 2009; 131:1384–1385. [PubMed: 19133723]
25. Marshall JD, Schnitzer MJ. *ACS Nano*. 2013; 7:4601–4609. [PubMed: 23614672]
26. Damiano MG, Mutharasan RK, Tripathy S, McMahon KM, Thaxton CS. *Adv. Drug Deliv. Rev*. 2013; 65:649–662. [PubMed: 22921597]
27. Li L, Daou T, Texier I, Chi T, Liem N, Reiss P. *Chem. Mater*. 2009; 21:2422–2429.
28. Deng D, Chen Y, Cao J, Tian J, Qian Z, Achilefu S, Gu Y. *Chem. Mater*. 2012; 24:3029–3037.
29. Pons T, Pic E, Lequeux N, Cassette E, Bezdetsnaya L, Guillemin F, Marchal F, Dubertret B. *ACS Nano*. 2010; 4:2531–2538. [PubMed: 20387796]
30. Li L, Pandey A, Werder DJ, Khanal BP, Pietryga JM, Klimov VI. *J. Am. Chem. Soc*. 2011; 133:1176–1179. [PubMed: 21207995]
31. Huang L, Zhu X, Publicover NG, Hunter KW Jr, Ahmadiantehrani M, de Bettencourt-Dias A, Bell TW. *J. Nanopart. Res*. 2013; 15:2056–2059.
32. Sun J, Yu Z, Hong C, Pan C. *Macromol. Rapid Commun*. 2012; 33:811–818. [PubMed: 22488562]
33. Yeh Y, Patra D, Yan B, Saha K, Miranda OR, Kim CK, Rotello VM. *Chem. Commun*. 2011; 47:3069–3071.
34. Aldeek F, Muhammed MAH, Palui G, Zhan N, Mattoussi H. *ACS Nano*. 2013; 7:2509–2521. [PubMed: 23394608]

Bioconjugatable zwitterionic QDs (ZW-QDs) were produced using lipid encapsulation.

The preparation of ZW-QDs is simple, fast, and cost effective.

The ZW-QDs are stable in solutions with high salinity and over a wide pH range.

The ZW-QDs can be applied for bioassay with low nonspecific binding.

The ZW-QDs may have broad biological and biomedical applications.

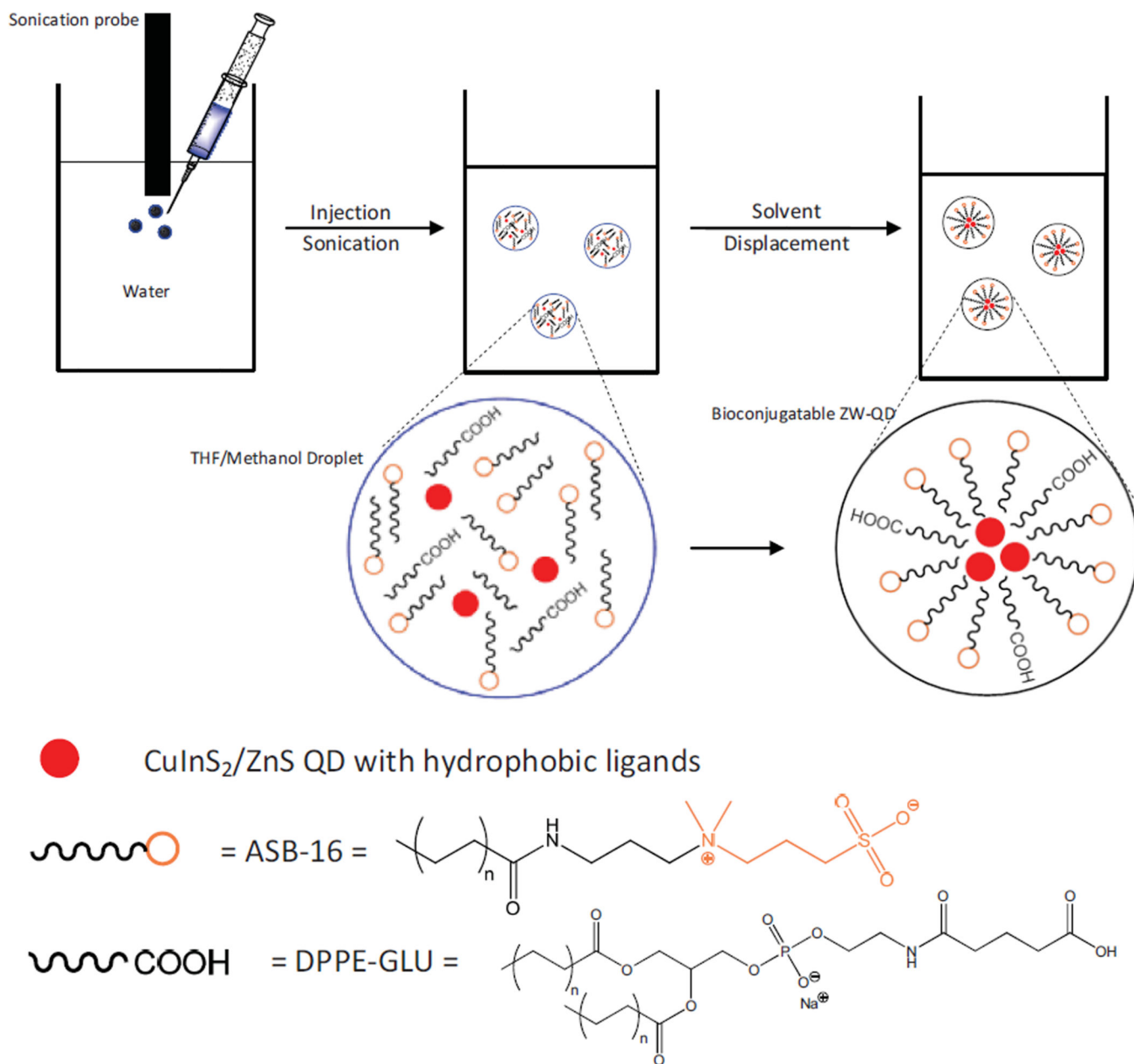


Figure 1.

Scheme of dual-lipid encapsulation for the preparation of bioconjugatable zwitterionic quantum dots (ZW-QDs) using ASB-16 lipid, DPPE-X lipid (X = amine, carboxyl, maleimide, etc. for bioconjugation), and $\text{CuInS}_2/\text{ZnS}$ QDs in a THF/methanol/water solvent system with sonication – After sonication, THF/methanol droplets containing QDs and lipids are formed and dispersed in water; highly water-soluble THF/methanol in droplets is displaced by water, which induces the self-assembly of lipids to ZW-QDs.

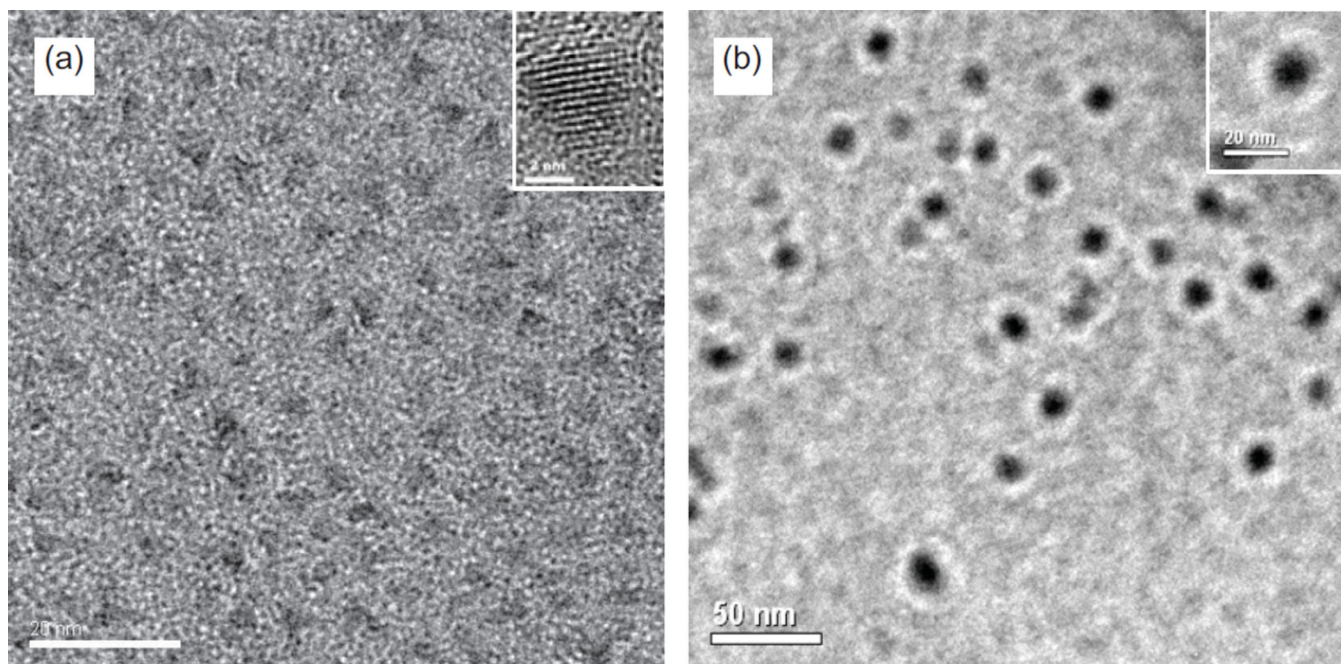


Figure 2.

(a) Representative TEM image of hydrophobic CuInS₂/ZnS QDs prepared in organic solvents; (b) Representative TEM image of zwitterionic CuInS₂/ZnS QDs after ASB-16 and DPPE encapsulation. The size of ZW-QDs is around 15 nm but that of hydrophobic QDs is around 5 nm.

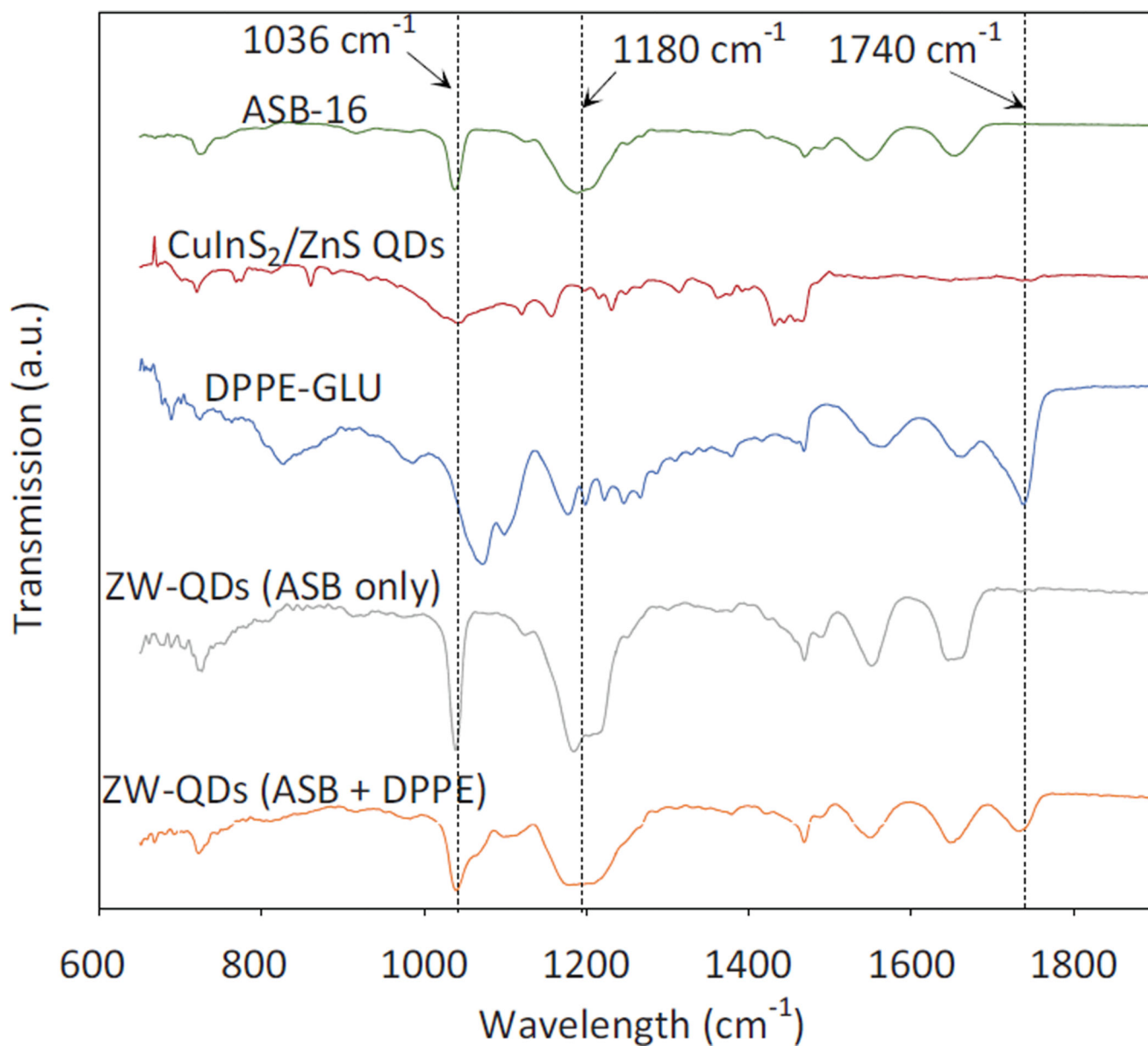


Figure 3.
FT-IR spectra of materials used in the synthesis of ZW-QDs and the produced ZW-QDs

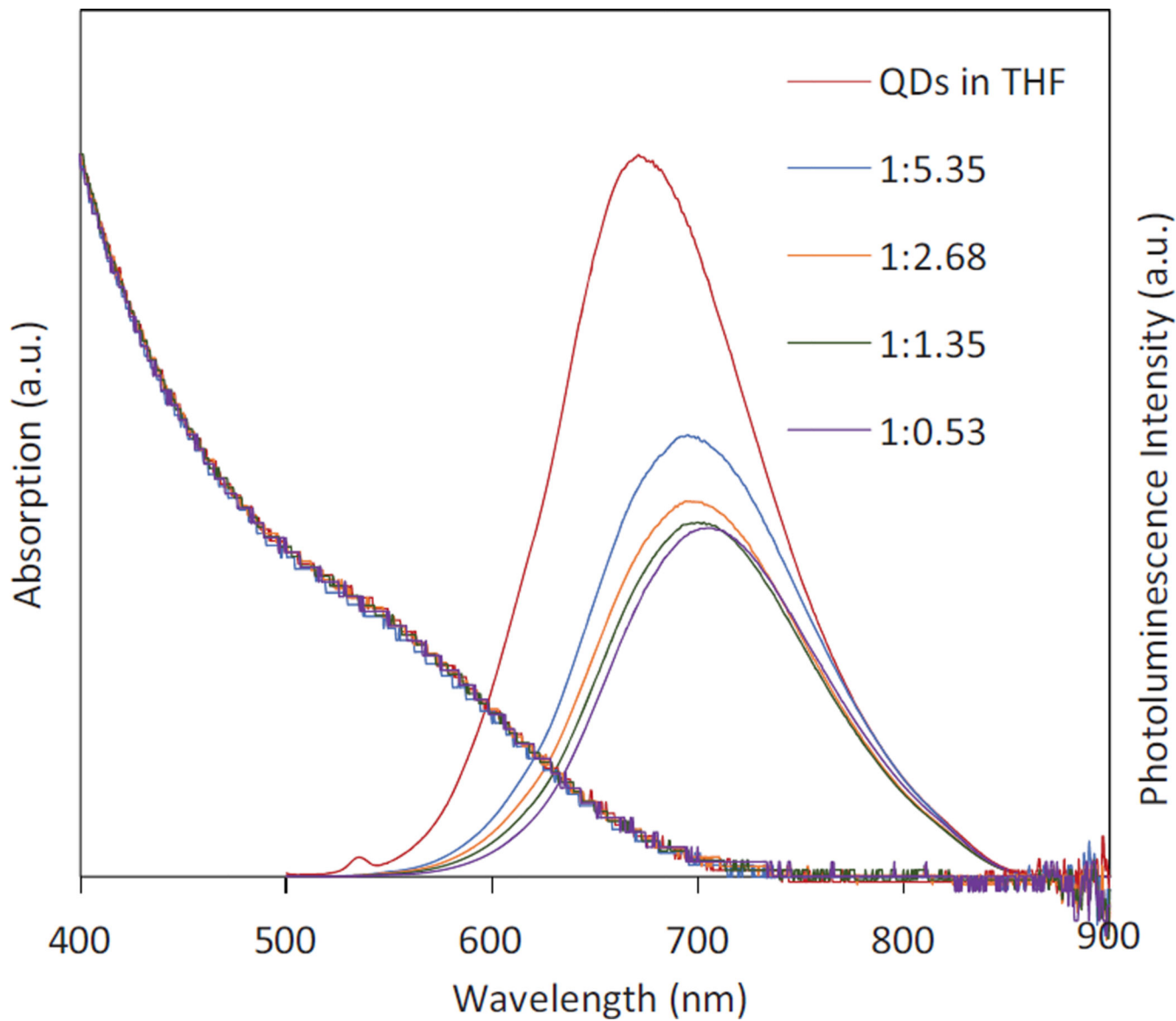
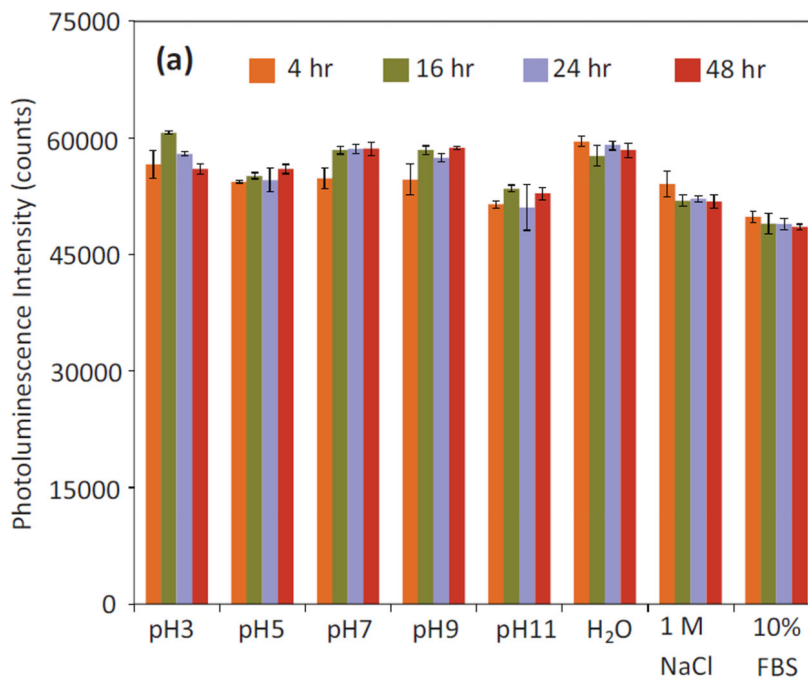
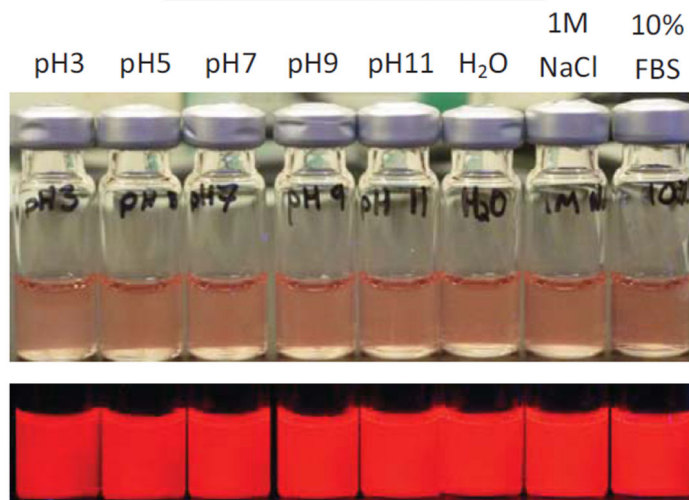


Figure 4. UV-Vis absorption and photoluminescence emission spectra of hydrophobic QDs in THF and ZW-QDs in water with the different mass ratios of QDs to the total lipids (ASB-16 and DPPE-GLU) used in the preparation process – the photoluminescence emission spectra are scaled to their relative quantum yields.



(b) pH and Salinity Conditions



Images of ZW-QDs in aqueous solutions

Figure 5.

(a) Photoluminescence intensity of the prepared ZW-QDs dispersed in PBS with pH 3–11, pure water, a 1M NaCl solution, and 10% FBS over 48 hours under room temperature; and (b) Photograph of the ZW-QDs after 48 hours under room temperature under the same conditions. The top panel image shows ZW-QDs in different solutions under room light, and the bottom panel is the photoluminescence image of ZW-QDs under 405 nm UV light.

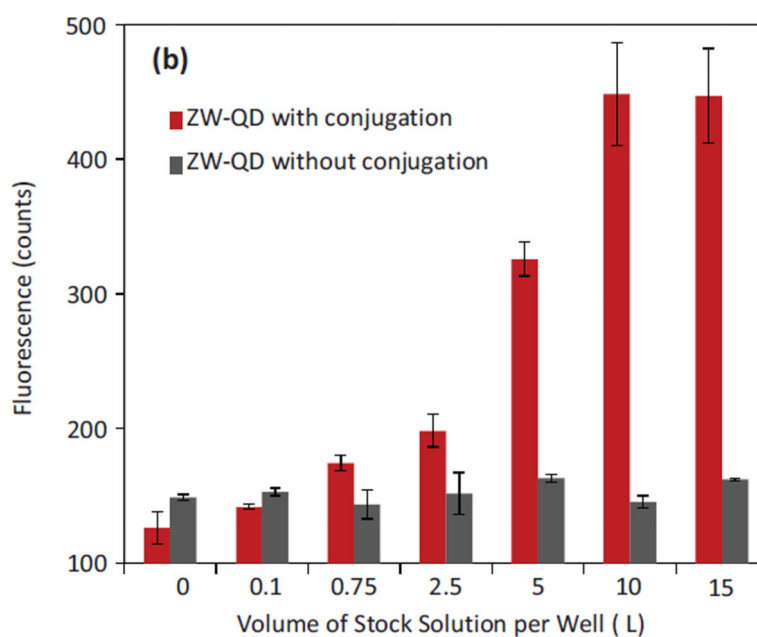
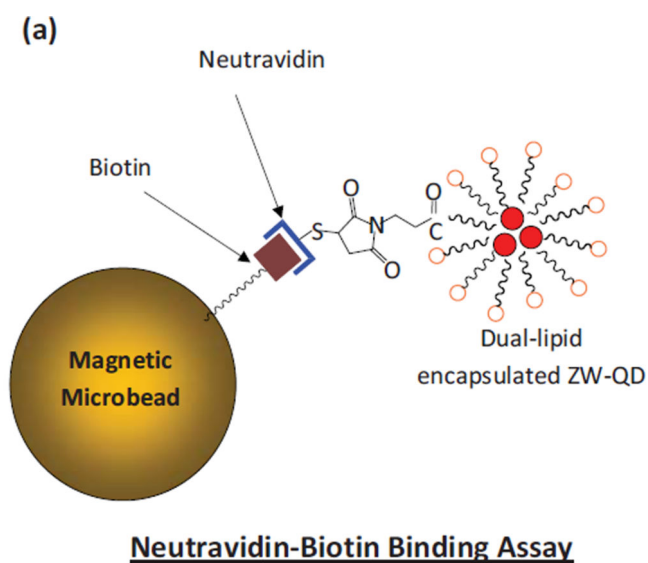


Figure 6.

(a) Illustration of Neutravidin-biotin assay using biotinylated magnetic microbeads and Neutravidin conjugated ZW-QDs; and (b) The photoluminescence responses to biotinylated magnetic microbeads after incubation with non-conjugated and Neutravidin conjugated ZW-QDs

Table 1

The starting material mass conditions for ZW-QD preparation

Hydrophobic QDs (mg)	ASB-16 (mg)	DPPE-GLU (mg)	Total Lipids (mg)	QD : Total Lipid Mass Ratio
0.6	2.22	0.99	3.21	1:5.35
0.6	1.11	0.5	1.61	1:2.68
0.6	0.56	0.25	0.81	1:1.35
0.6	0.22	0.099	0.319	1:0.53